

Article

Not peer-reviewed version

Influence of Metal Magnesium Addition on Detonation Initiation in Shock Wave Focusing

Yu-Peng Hu , Yun-Tian Zhang , Peng Du , [Rui Xue](#) ^{*} , Yi-Jun Wang , Ben-Quan Zhou

Posted Date: 30 May 2023

doi: 10.20944/preprints202305.2062.v1

Keywords: Magnesium particle; Shock wave focusing; Detonation wave; DDT



Preprints.org is a free multidiscipline platform providing preprint service that is dedicated to making early versions of research outputs permanently available and citable. Preprints posted at Preprints.org appear in Web of Science, Crossref, Google Scholar, Scilit, Europe PMC.

Copyright: This is an open access article distributed under the Creative Commons Attribution License which permits unrestricted use, distribution, and reproduction in any medium, provided the original work is properly cited.

Article

Influence of Metal Magnesium Addition on Detonation Initiation in Shock Wave Focusing

Yu-Peng Hu ^{1,2}, Yun-Tian Zhang ², Peng Du ², Rui Xue ^{2,*}, Yi-Jun Wang ¹ and Ben-Quan Zhou ¹

¹ Institute of systems Engineering, China Academy of Engineering Physics, Mianyang 621999, China

² State Key Laboratory for Strength and Vibration of Mechanical Structures, Shaanxi Engineering Laboratory for Vibration Control of Aerospace Structures, School of Aerospace, Xi'an Jiaotong University, 710049 Xi'an, People's Republic of China

* Correspondence: ruixue@xjtu.edu.cn

Abstract: The process of shock wave focusing can make the strength of shock waves be continuously accumulated and turned into detonation wave in Pulse Detonation Engine (PDE). However, its effective application needs the inlet jets be in high temperature and velocity, which is difficult to be satisfied under certain conditions. Therefore, in this paper, metal magnesium assisted detonation initiation is proposed and the effect of magnesium particle addition on the shock wave focusing process in a kerosene-fueled PDE with cavity configuration is investigated through numerical simulation. The result showed that when the temperature of the premixed fuel/air jets injected in opposite direction was set as 650 K, the collision of leading shock waves on the central axis was the main source of energy deposition and the shock wave focusing could make the detonation be initiated in the cavity. When the temperature of jets is reduced to 550 K, fuel ignition and detonation could not be achieved through shock wave focusing. Then adding metal magnesium particles into the combustor made the energy deposition be enhanced and the detonation be induced. The diffusion of metal particles can significantly change the structure, motion, merging and dissipation of vortices in the flow field. Generally, the shock wave focusing process is basically not affected with metal particles injection. Therefore, this method can be successfully employed for detonation initiation in the cavity when the fuel/air premixed jet temperature is not high for PDE.

Keywords: magnesium particle; shock wave focusing; detonation wave; DDT

1. Introduction

Compared with deflagration, detonation combustion has the advantages of self-pressurization and a fast combustion rate. In general, Detonation waves can be induced by deflagration-to-detonation (DDT) or direct initiation [1–3]. Indirect detonation needs lower energy density and it is a DDT process through the effect of various nonlinear instabilities phenomenon. Such the electric fuse blown ignition method which is difficult to achieve is often employed to induce direct detonation. In a high-speed flow, a shock wave forms after a strong compression process when the flow velocity exceeds the local speed of sound [4,5]. Aiming at this key problem, Levin [6] proposed to utilize the high-energy region generated by the shock wave focusing method to trigger detonation. This method is a direct ignition method that does not require additional ignition devices. Compared with other detonation methods, shock wave focusing has greater advantages in high energy efficiency. In the actual process, the detonation failure will occur because the impact of the inlet jet cannot provide adequate energy.

Therefore, powder fuels with low volatility and relatively stable physical and chemical properties can effectively contribute to the understanding of detonation physics. Many scholars have carried out numerical and experimental studies on this before and obtained some preliminary conclusions. Alien J. Tuli and J. Robert Selman [7] performed detonation experiments of aluminum particles in a cavity without space constraints, and obtained the effect of particle surface mass ratio on the detonation process. The initial detonation law of aluminum particles in unrestricted space is obtained. Bernard Veyssiere [8] conducted an experimental study on the detonation process of

aluminum particles in vertical detonation, and observed a double-peak detonation wave phenomenon. Sergey Lavruk [9] proposed a mathematical model to describe the kinetics of the mixing of inhomogeneous aluminum particles in gas phase detonation. The analytical results are in good agreement with the experimental data. B. Veyssiere [10] proposed a simplified model for the initiation of aluminum particles. The numerical results successfully predict the ignition delay time, which is in good agreement with the experimental values. T. Hsieh [11] studied the effect of adding octogen (HMX) in the process of gas phase deflagration to detonation by numerical simulation method. The numerical results are in good agreement with the experiments. Yiguang Ju [12] applied theoretical derivation and numerical simulation to analyze the process of bending detonation wave passing through gas mixture with particles. An expression is obtained that describes the combined effects of heat and momentum losses due to particle interaction with the gas phase and wave curvature on detonation velocity. Numerical simulation results show that particle heat loss, momentum loss, and wave curvature significantly reduce the detonation velocity, causing detonation quenching. When the particle volume fraction is fixed, the gas phase heat loss with smaller particles is larger, the detonation velocity is lower, and the detonation range is smaller.

Metal powders such as aluminum and magnesium as fuels have high calorific value and the advantage of easy storage. Compared with metal magnesium, aluminum has a higher energy density. However, due to the lower melting point and boiling point of magnesium, it has better ignition characteristics and combustion efficiency so that it can be expected to play a key role in the ignition process [13]. Kofstad P [14] pointed out that the oxides on the surface of magnesium are porous so that the oxide film does not protect the magnesium inside. The oxidation rate of magnesium is independent of the quality of oxide formation. E. A. Gulbransen et al. [15] conducted an experimental study and found that the oxidation reaction and vaporization of magnesium can be observed simultaneously even in the state of magnesium solid. G. K. Ezhovskii et al. [16] conducted an experimental study on the chemical reaction rate of magnesium particles with and without the vaporization endotherm. The result shows that the heat loss of metal evaporation does not need to be considered when studying the combustion limit. Abbud Madrid A et al. [17] carried out experimental and numerical simulation studies. The chemical kinetic model was obtained for gaseous magnesium with oxygen or carbon dioxide considering condensation.

In this paper, combined with the combustion characteristics of magnesium, the method to inject magnesium powders is proposed for the problem that detonation failure in the process of shock focusing process. Numerical studies were carried out on the detonation-assisting process of magnesium particles and the interaction of particles and shock focusing.

2. Numerical Methods and Validation

In this paper, the governing equations solved are unsteady two-dimensional compressible Navier-Stokes (N-S) equations and the k- ω SST model is employed to close the equations. The finite volume method is employed for discretization and the particle ejection was performed using the DPM model. The governing equations are:

$$\frac{\partial \rho}{\partial t} + \nabla \cdot (\rho \mathbf{U}) = 0 \quad (1)$$

$$\frac{\partial (\rho \mathbf{U})}{\partial t} + \nabla \cdot (\rho \mathbf{U} \mathbf{U}) + \nabla P + \nabla \cdot \hat{\tau} = 0 \quad (2)$$

$$\frac{\partial E}{\partial t} + \nabla \cdot ((E + P) \mathbf{U}) + \nabla \cdot (\mathbf{U} \cdot \hat{\tau}) + \nabla \cdot (K \nabla T) + \rho q \dot{\omega} = 0 \quad (3)$$

$$\frac{\partial (\rho Y)}{\partial t} + \nabla \cdot (\rho Y \mathbf{U}) + \nabla \cdot (\rho D \nabla Y) - \rho \dot{\omega} = 0 \quad (4)$$

$$P = \rho RT/M \quad (5)$$

Here ρ denotes the density, \mathbf{U} is the velocity, P is the pressure, $\hat{\tau}$ is the viscous stress tensor. E stands for the energy density, K is the thermal conduction coefficient, T is the temperature, and q is the total chemical energy release, $\dot{\omega}$ is the reaction rate, Y is the mass fraction of reactant, D is the mass diffusivity and M is the molecular weight.

E is determined by the enthalpy H :

$$E = H - P/\rho \quad (6)$$

where

$$H = h - |\mathbf{U}|^2/2 \quad (7)$$

Previous studies have proved that the application of the global reaction mechanism in the detonation problem is effective and feasible, and this can greatly improve the computational efficiency. Therefore, the finite rate model is adopted for the fuel combustion reaction simulation, and the global reaction mechanism of $C_{12}H_{23}/Air$ is employed. The reaction rate is determined by Arrhenius' law:

$$\frac{dY}{dt} = \dot{\omega} = -A\rho Y \cdot \exp(-E_a/RT) \quad (8)$$

where $A = 2.587 \times 10^9 s^{-1}$ is the pre-exponential factor. T is the temperature, $E_a = 1.256 \times 10^8 J/kmol$ is the activation energy of reaction and R is the universal gas constant. The chemical reaction of magnesium particles is divided into surface reaction and gas-phase reaction, and they are all one-step reactions, the chemical reaction rate is related to the physical state of magnesium particles. This paper assumes that after the temperature of magnesium particles reaches the ignition point, there will be gas-phase magnesium precipitation, and before reaching the ignition point, only surface reactions occur on the magnesium particles. The rate of oxygen consumption is:

$\dot{\omega} = 1.79 \times 10^9 Y_{O_2,s} \exp(-170000/RT_p)$; For gas phase reaction, the oxygen consumption rate in this reaction is: $\dot{\omega} = 1.05 \times 10^8 \exp(-69010/RT_g)(\rho_g^2/M_{Mg})Y_{O_2}Y_{Mg}$. For this reaction rate, magnesium oxide is applicable to both gas phase and condensate phase. Wang [20] conducted an experimental study and found that for magnesium with a particle size of 1-11 μm , the average thickness of the oxide layer reaches 3.4 μm under an air environment. Therefore, in this paper, 30% of the particles were considered as consumption for surface chemical reactions and the rest as vaporizable mass. Shoshin Y et al. [21] conducted an experimental study on the volatilization rate of magnesium particles at high temperatures. The volatility coefficients for magnesium particles employed in this paper depends on the flame temperature of the flow field.

For verifying the accuracy of the numerical method, the shock-induced combustion experiment was selected as the validation case [22]. In this experiment, a high-speed spherical projectile with a diameter of 15 mm was shot into the stoichiometric hydrogen/air mixture at a pressure of 46626 Pa and a temperature of 286.6 K. The reaction mechanism adopts the 9 component/27 reaction steps hydrogen-air chemical reaction kinetic model established by Marinov, which has been proved feasible in high-speed flow [23].

Figure 1 shows the temperature distribution in front of and behind the wave obtained by this numerical simulation. The dots mark the position of the detonation wave in the experiment. Compared with the experimental data, the numerical results have successfully captured the detonation wave structure in front of the head of a high-speed projectile.

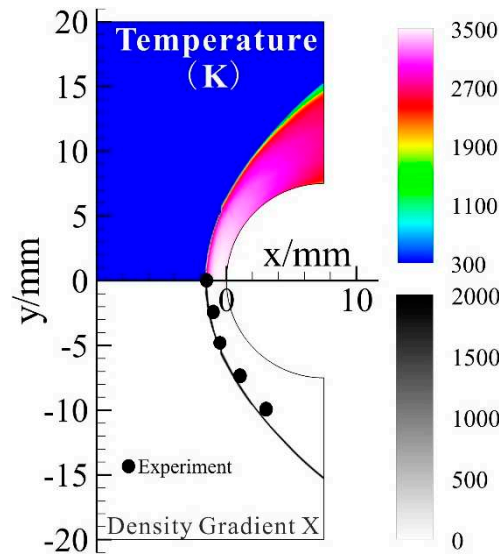


Figure 1. Temperature distribution contour and comparison with experimental points.

Compared with deflagration, the typical characteristic of detonation is that the flame front couple with the shock wave. The pressure and temperature distribution along $y=0$ mm through the wave surface is shown in Figure 2. The position of jumps in temperature and pressure induced by the wave is coincident, marking the formation of a detonation wave. Furthermore, the chemical reaction takes place over a short distance and reactants behind the detonation wave almost run out. This phenomenon is consistent with the theory that the reaction rate on the detonation wave is infinite. Overall, this validation proves that the numerical method employed in this paper is appropriate for the simulation of shock wave/flame interaction and ignition-initiation process. Therefore, it is reasonable to apply the simulation method to the subsequent shock focusing and detonation process.

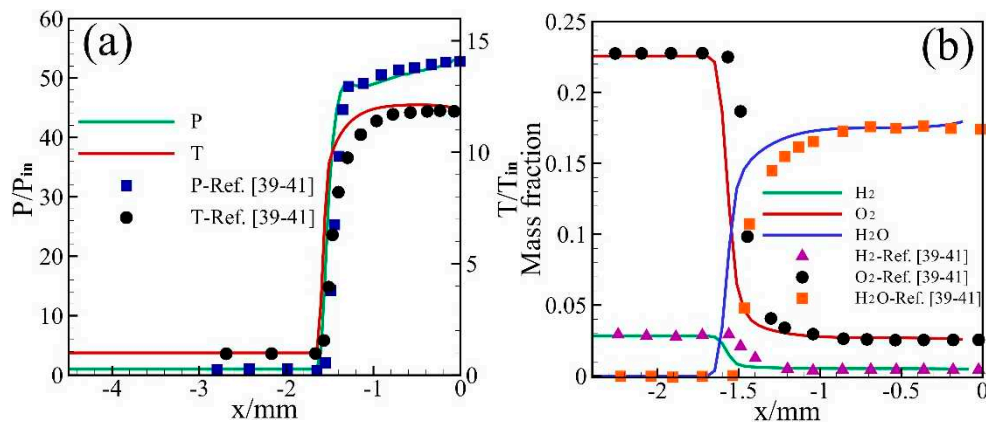


Figure 2. The verification of thermodynamic parameters on $y=0$ mm [24–26].

Physical Models and boundary condition

Figure 3 shows the model engine configuration which has two axisymmetric inlets. It consists of a semicircular cavity with a radius of 60mm and an equal-straight detonation wave propagation channel with a length of 150mm. Fuel/air mixtures fed into the cavity through two inlets with a diameter of 10 mm. Due to the symmetry of the physical model, only half of the region is employed as the computational domain to improve efficiency.

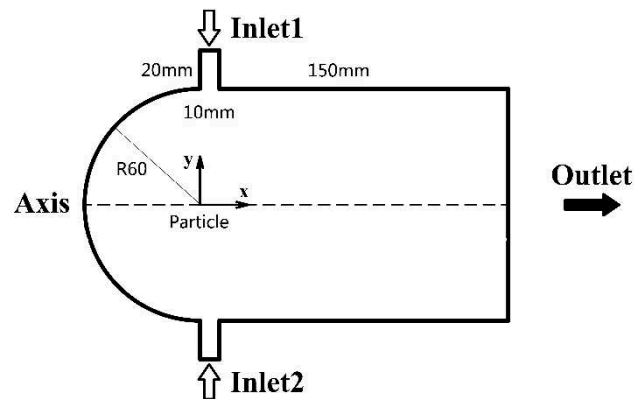


Figure 3. Geometric physical configuration (Unit: mm).

For studying the effect of metal powder fuel on detonation, three cases with different inlet conditions are set up in this paper as shown in Table 1. The inlet pressure is $P_{in}=150$ kPa, the inlet flow rate is $Ma_{in}=2$, and the jet is kerosene/air premixed gas with a stoichiometric ratio of 1. The outlet pressure is 1 atm. Two jet temperatures which are 650 K and 550 K respectively are chosen to investigate whether the jet temperature can influence the shock wave focusing and detonation initiation. The diameter of the added magnesium particles is set as $5\text{ }\mu\text{m}$, and its total mass is 0.15 g for 550K inlet jets. Magnesium particles are placed at the center of the left semicircle, and their velocity is zero. As for mesh, there are more than 200,000 grids. The initial flow field temperature is the same as that of air flow, and the pressure is atmospheric.

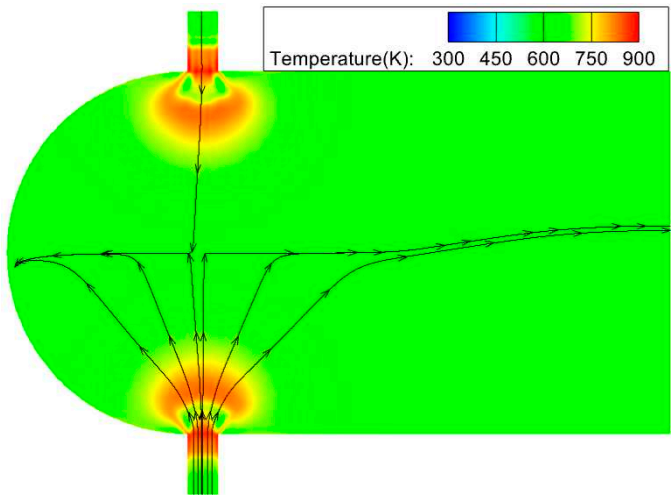
Table 1. Cases and the result of detonation.

Parameters	Case1	Case2	Case3
Jet temperature/K	650	550	550
Particles	N	N	Y
Detonation	Y	N	Y

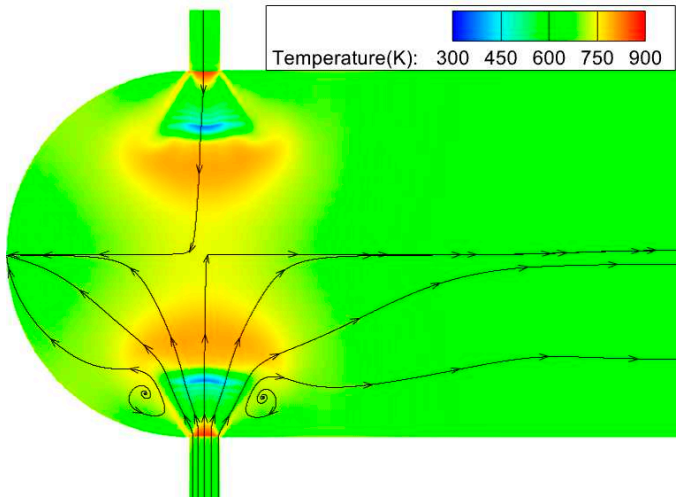
3. Results and discussion

3.1. Effect of jet temperature without metal powder addition

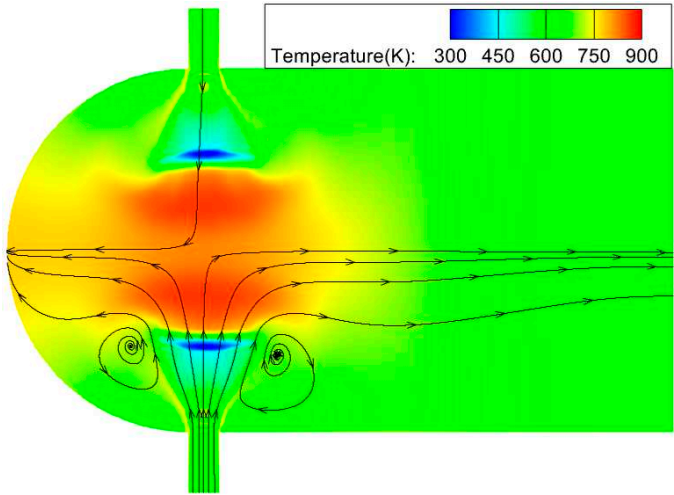
Figure 4 shows the temperature and pressure evolution of the flow field at the initial stage as the jets are fed into the combustor. It can be seen that when the jets are injected into the combustor, the leading shock waves in front of the jets are formed and move to the central axis. The temperature behind the waves is increased to about 750K, which is not high enough for fuel ignition. At $t=0.1$ ms, two vortex structures were formed on both sides of jets near the inlets (Figure 4b). As shown in Figure 4d, the area of the low-pressure region behind the vortex structure increases with the movement of shock waves, and both the temperature and pressure in the central region continue to rise correspondingly. As the leading shock wave continues to move forward to the central axis, they approached at $t=0.15$ ms and the temperature at the axis increased significantly to 850 K. In addition, an obvious high-pressure region is formed as the leading shock waves collide to each other, which induces the left-travelling and right-travelling shocks waves (Figure 4e).



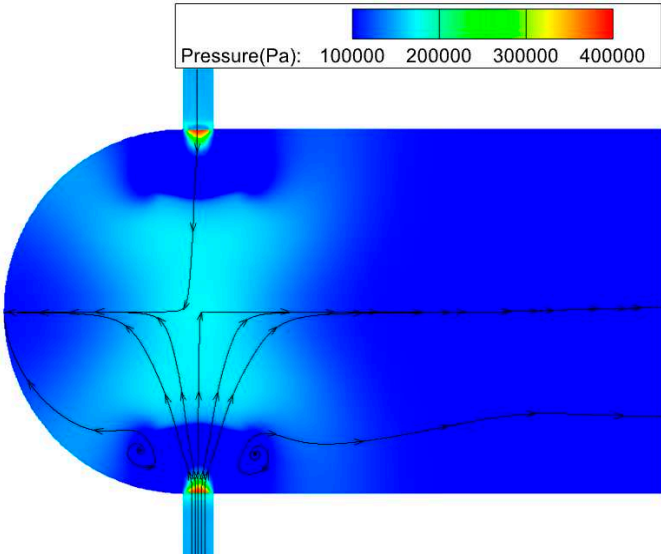
(a) Temperature at $t=0.05\text{ms}$



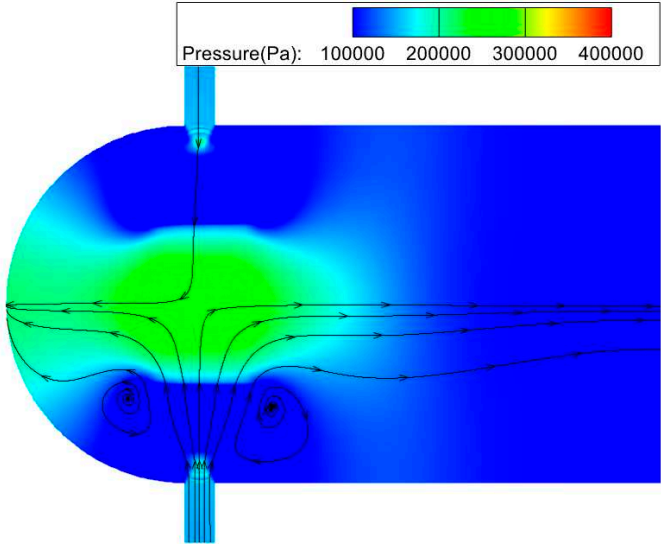
(b) Temperature at $t=0.1\text{ms}$



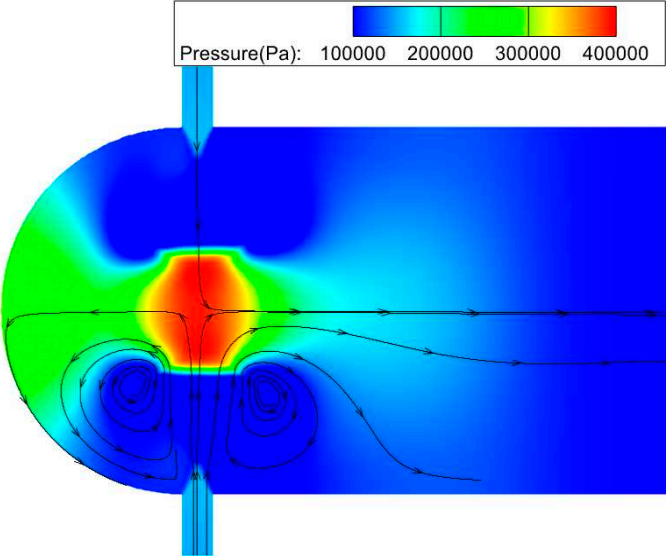
(c) Temperature at $t=0.15\text{ms}$



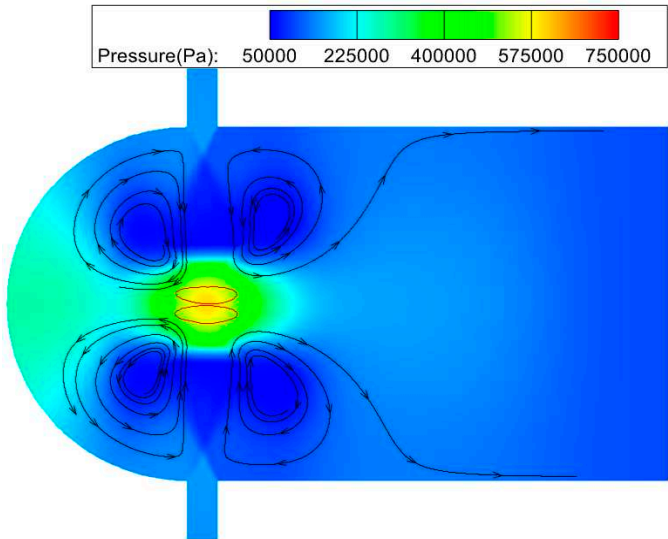
(d) Pressure at $t=0.1\text{ms}$



(e) Pressure at $t=0.15\text{ms}$



(f) Pressure at $t=0.2\text{ms}$

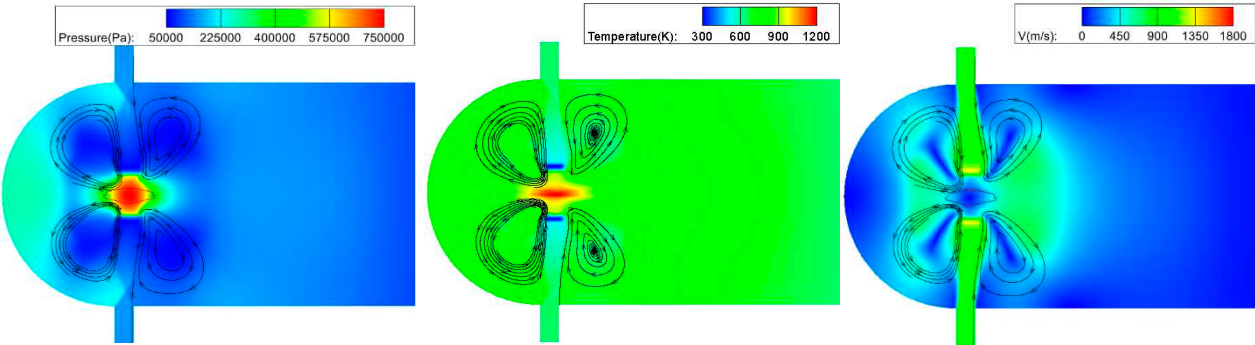


(g) Pressure at t=0.22ms

Figure 4. Temperature and Pressure distribution before detonation initiation for 650K jet temperature.

At t=0.2ms shown in Figure 4f, a high-pressure region is generated in the core flow and expands to the cavity bottom wall due to the compression induced by wall confinement and the jets. Meanwhile, the right-travelling shock wave moves toward the outlet, and also creates a high-pressure region near the outlet wall. At t=0.22 ms in Figure 4g, the pressure in the cavity further increases and the temperature of the regions near the central axis reaches as high as 1000K.

As shown in Figure 5a, when the two high-energy regions are combined, the temperature is increased to as high as 3500 K and the pressure reaches highest in the collision point at t=0.25ms, which makes the fuel ignition and detonation is initiated. The formed flame surface is squeezed by the jet and expands in a flat shape. It can be seen that the impact of jets causes the gas in the center to be continuously compressed and forms a barrier that restricts the propagation of the flame to the direction of the incoming flow from the inlet at t=0.25ms.



(a) t=0.25ms

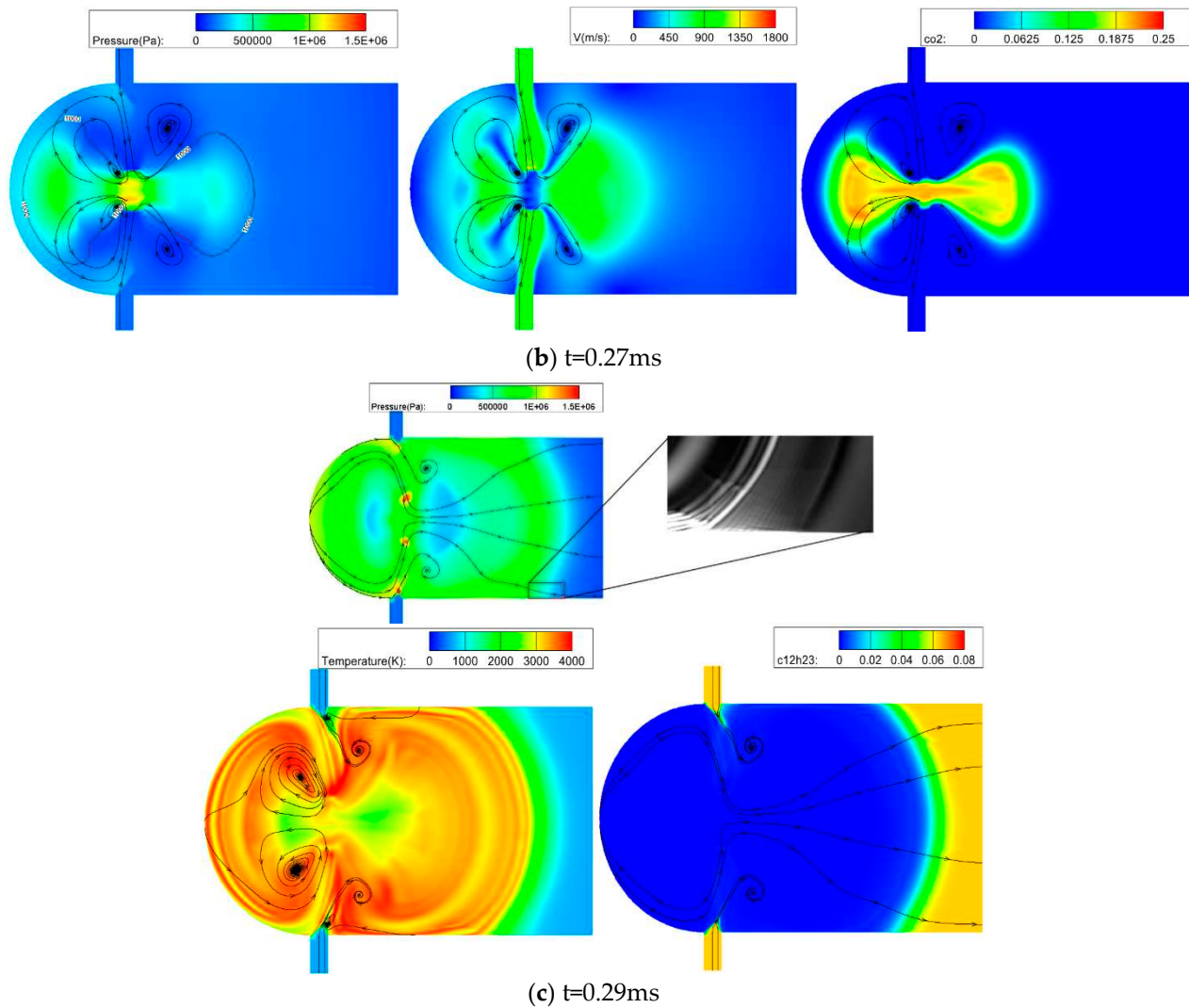


Figure 5. Flow field structure from $t=0.25\text{ms}$ to $t=0.29\text{ms}$.

At $t=0.27\text{ms}$, four large-scale vortices are formed in the low-velocity region. Due to the cooling effect with jet injection, the reaction region is dispersed, and the reaction product CO_2 is pushed forward to the cavity and the exit, respectively. Compared with the flow structure at $t=0.25\text{ms}$, the left vortex moves closer to the center due to the formation of the high-pressure region induced by the detonation wave at $t=0.27\text{ms}$, and the right vortex deviates from the central area because of the jet interference.

At $t=0.29\text{ms}$, when the detonation wave collides to the cavity bottom wall, it then propagates backward and a large amount of combustion products are generated. In Figure 5c for temperature distribution, it can be seen that with the detonation initiation, fuel is ignited and most part of the combustor are in high temperature. In addition, the injected jets not only induce a vortex structure be produced between the jet and the Mach stem but also collide to the detonation wave to form another set of vortex structures. Thus, the total number of vortex structures has been increased from 4 to 6 at this moment. The premixed gas enters the cavity again at $t=3.5\text{ms}$ (Figure 6a). The exist of the vortex structure cause the newly entering unburned gas to flow in a specific direction. This can inhibit the emission of combustion products to the outlet at some extent.

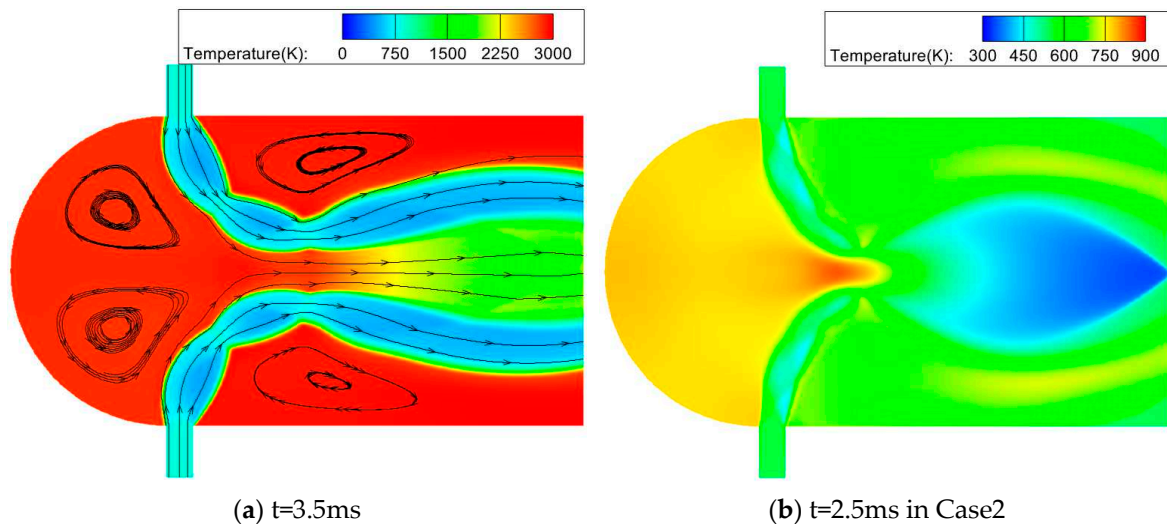


Figure 6. Temperature distribution at $t=3.5\text{ms}$ and at $t=2.5\text{ms}$ in Case2.

When the temperature of the jet is reduced to 550 K, though with the shock wave focus process both the temperature and the pressure of the injected fuel/air mixture can be enhanced, the increased energy is not enough to induce detonation and fuel ignition (Figure 6b). Therefore, based on the research of shock wave focusing with different jet temperatures (Case1 and Case2), it can be concluded that the ignition and detonation may not be triggered in shock wave focusing process if the temperature of the injected fuel/air jets is not high enough under a certain cavity configuration. The energy deposition produced by shock focusing with the use of lower temperature jet is insufficient to achieve ignition and detonation. Therefore, other suitable auxiliary methods need to be employed to make the detonation initiated in the combustor.

3.2. Effect of metal powder addition on shock wave focusing

In order to explore whether the addition of high energetic metal powder can help and improve the start of detonation when the temperature of the injected fuel/air mixture is not high, a mass flow of 0.5 kg/s magnesium powder is added into the combustor under the 550 K jet temperature condition (Case 3). As shown in Figure 7, the injection of magnesium particles can obviously affect the flow field characteristics. At $t=0.11\text{ ms}$, the leading shock waves collide on the axis to form a high pressure region. Due to the low velocity inside this region, the metal particle did not diffuse broadly during the collision. The generated left-traveling shock wave moves toward the left semicircular wall and is gradually converged. When it collides with the left wall, the effect the shock wave focusing induce a high-pressure spot be generated and a secondary collision shock wave is formed (Figure 7b). Then this secondary shock wave spreads from the collision point to the surrounding fluids. After it collides with the inlet jets, another two high-pressure areas are produced close to the left side of the jets at $t=0.29\text{ms}$ (Figure 7c). At this stage, the added magnesium powder basically has no strong interaction to the flow and ignition.

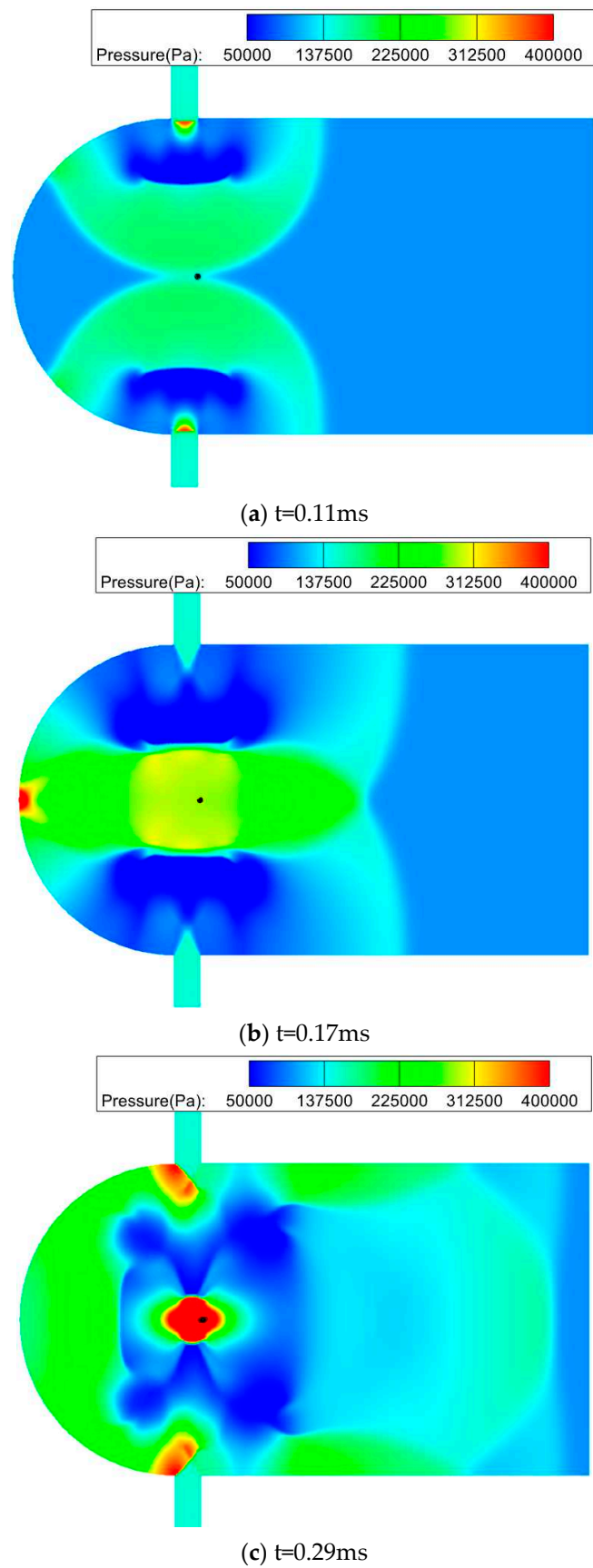


Figure 7. Pressure changes under leading shock focusing process.

As shown in Figure 8, when the secondary shock wave spreads to the outlet, four small vortices are generated in the central area at $t=0.31\text{ms}$. As the injected jets do not arrive to the central region,

the two small vortices on the left side are gradually absorbed by the two large vortex structures in the semicircular region. This can make the magnesium powder particles to diffuse widely in the flow field. In Figure 8c, as the small vortices are completely merged to a larger vortex, a high pressure gradient zone appears on both sides of the magnesium powder particle cluster. This causes the magnesium powder particles to move and spread to the left side of the combustor, as shown in Figure 9a ($t=0.4\text{ms}$).

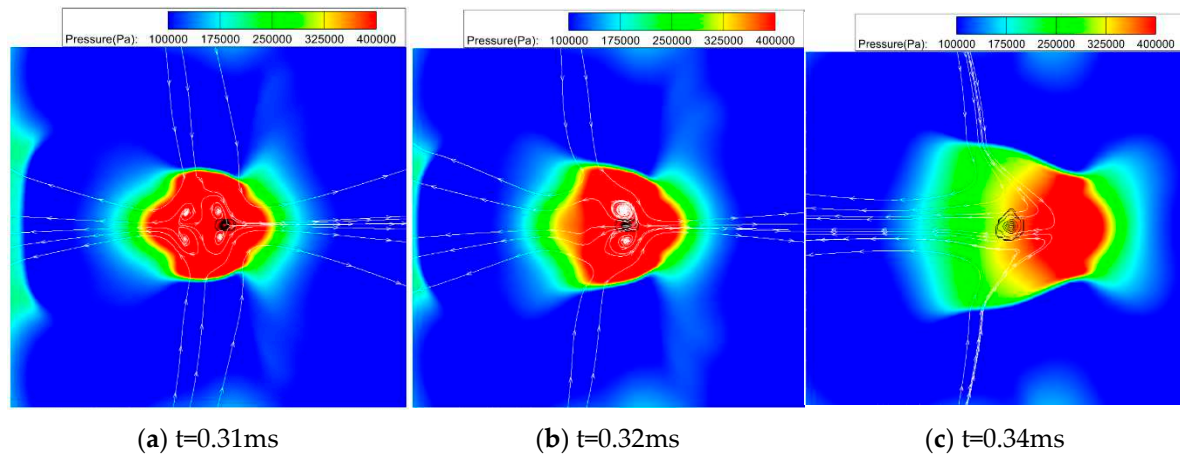


Figure 8. Pressure changes in the collision zone of the leading shock.

In Figure 9b at $t=0.57\text{ms}$, the magnesium powder particles are gradually dispersed in the process of moving to the left. Driven by the left two vortex, they gradually gather together at the bottom of the cavity and move along the semicircular wall surface. At last, they moved to the jet near the semicircular wall surface. After the intersection of the two jet streams at the axis, most of the particles return to the semicircular area and the other particles move towards the exit.

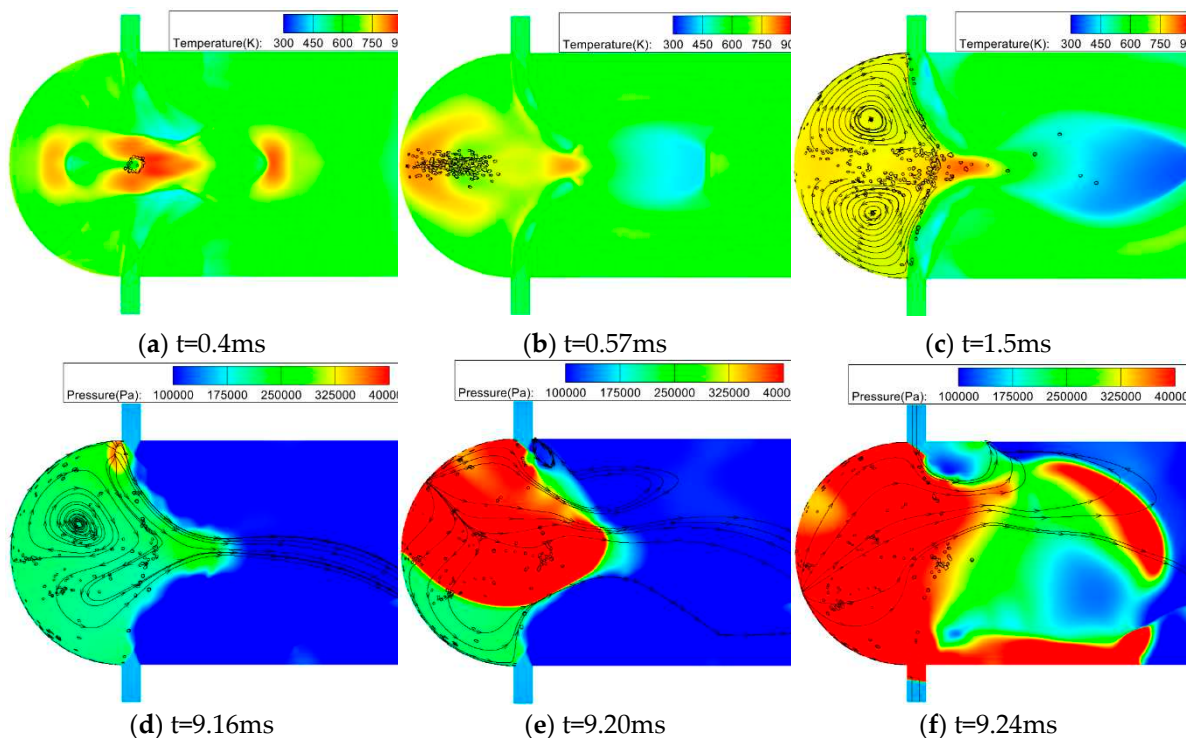


Figure 9. Temperature distribution and particle location during particle diffusion.

At $t=9.16\text{ms}$ (Figure 9d), detonation is triggered which make a high-pressure and temperature region be produced at the top of semicircular wall near the inlet. Then the newly formed detonation

wave quickly sweeps across the cavity and rapid chemical reaction occurs with the magnesium particles scattered in the flow. Compared to the shock wave focusing and detonation initiation under higher temperature inlet jets, the method of magnesium powder assisted detonation at relatively low temperature jet leads to a certain ignition delay in the start of detonation. The transient processes of magnesium powder-assisted detonation initiation can be illustrated in Figure 9e from $t=9.2$ ms to $t=9.24$ ms. Under the influence of jets, the detonation wave sweeps across the entire semicircular area from top to bottom. Meanwhile, the original vortex structure is rapidly destroyed and causes a rapid increase in the pressure gradient, which even drives part of the flame to block the inlet jets. After this, the detonation wave continues to move towards the exit and gradually turns into a shock wave. During this process, the temperature of the burned gas in the cavity can reach as high as 3000 K, which means violent chemical reaction and heat release occur in the engine.

Therefore, it can be seen that the addition of magnesium particles has a positive effect on the detonation initiation during the shock wave focusing process especially for the relatively low jet temperature case. The position of the detonation start depends on where the magnesium particles are added. For the combustor configuration and the operating condition employed in this paper, detonation is triggered near the intersection of the inlets and the semicircular wall.

4. Conclusion

In this paper, the numerical simulation is employed to study the shock focusing process under the pure gas-phase jet and the effect of magnesium particles addition for detonation initiation under relatively lower temperature jets. The basic conclusions are as follows:

When the temperature of the premixed fuel/air jets injected in opposite direction is set as 650 K, the shock wave formed by the jet collision in the central axis can lead to a large amount of energy be deposited in a small region and the initiation of detonation through the shock wave focusing process in the cavity. The collision of leading shock waves on the central axis is the main source of energy deposition. However, when the temperature of jets is reduced to 550 K, fuel ignition and detonation are difficult to be induced only relying on shock wave focusing process.

Adding metal magnesium particles into the cavity can improve the energy deposition level and facilitates the occurrence of detonation initiation as the premixed injecting jets are in lower temperature. The diffusion of metal particles can significantly change the structure, motion, merging and dissipation of vortices in the flow field. However, the process of shock wave focusing is not influenced a lot with metal particles addition, while the position of detonation initiation altered. Thus, adding high calorific value metal fuel can effectively promote the energy deposition during shock wave focusing, and this method can be used to achieve successful detonation initiation in the combustor as the jet temperature is not high.

Acknowledgments: This work was financially supported by China Postdoctoral Science Foundation (Grant No. 2019TQ0246, 2019M663734), the National Science Basic Research Program of Shaanxi (Program No. 2022JM-231).

Declaration of conflicting interests: The authors declare that there is no conflict of interest.

References

1. Wang, J.; Zhao, X.; Gao, L.; Wang, X.; Zhu, Y. Effect of solid obstacle distribution on flame acceleration and DDT in obstructed channels filled with hydrogen-air mixture. *Int. J. Hydrog. Energy* 2022, 2, 35. <https://doi.org/10.1016/j.ijhydene.2022.02.035>.
2. Gamezo, V.N.; Bachman, C.L.; Oran, E.S. Effects of Scale of Flame Acceleration and DDT in Obstructed Channels, AIAA Scitech 2020 Forum, American Institute of Aeronautics and Astronautics, 2020.
3. Li, M.; Liu, D.; Shen, T.; Sun, J.; Xiao, H. Effects of obstacle layout and blockage ratio on flame acceleration and DDT in hydrogen-air mixture in a channel with an array of obstacles. *Int. J. Hydrog. Energy* 2022, 47, 5650-5662. <https://doi.org/10.1016/j.ijhydene.2021.11.178>.
4. Urzay, J. Supersonic Combustion in Air-Breathing Propulsion Systems for Hypersonic Flight. *Annu. Rev. Fluid Mech.* 2018, 50, 593-627. <https://doi.org/10.1146/annurev-fluid-122316-045217>.
5. Teng, H.H.; Zhang, D.L.; Li, H.H. Numerical investigation of detonation direct initiation induced by toroidal shock wave focusing. *Explos. Shock. Waves* 2005, 25, 512-518.

6. Levin, V.A.; Nechaev, J.N.; Tarasov, A.I. A new approach to organizing operation cycles in pulse detonation engines, *High-Speed Deflagration and Detonation: Fundamentals and Control*, 2001, pp. 223-238.
7. Alien J. Tuli, J. Robert Selman. Unconfined Aluminum Particle Two-Phase Detonation in Air, *Dynamics of Shock Waves, Explosions, and Detonations*. January 1985. 277-292.
8. Bernard Veyssiere. Double-Front Detonations in Gas-Solid Particles Mixtures, *Dynamics of Shock Waves, Explosions, and Detonations*. January 1985. 264-276.
9. Khmel, T., and Lavruk, S. Detonation flows in aluminium particle gas suspensions, inhomogeneous in concentrations, *Journal of Loss Prevention in the Process Industries* Vol. 72, 2021, p. 104522.
10. B. Veyssiere. Ignition of Aluminum Particles in a Gaseous Detonation, *Shock Waves, Explosions, and Detonations*. January 1983. 362-375.
11. T. HSIEH and K. KIM. Numerical simulation of a complete deflagration-to-detonation transition process in porous beds of HMX particles, *AIAA 1990-153. 28th Aerospace Sciences Meeting*. January 1990.
12. Yiguang Ju and Chung Law. Detonation propagation and quenching in gas-particle mixtures, *AIAA 2001-477. 39th Aerospace Sciences Meeting and Exhibit*. January 2001.
13. LIU Long. Investigations on the Characteristics of Ignition and Self-maintenance Combustion of Powdered Fuel Ramjet Charged with a Mixture of Magnesium and Boron. National University of Defense Technology, 2014.
14. Kofstad P, Steidel C A. High Temperature Oxidation of Metals. *Journal of The Electrochemical Society*, 1967, 114(7):196-203.
15. Gulbransen E. The Kinetics of Oxide Film Formation on Metals and Alloys. *Physiologia plantarum*, 1947. <https://doi.org/10.1149/1.3071793>.
16. Ezhovskii G K , Ozerov E S . Combustion of powdered magnesium. *Combustion, Explosion and Shock Waves*, 1977, 13(6):716-721. <https://doi.org/10.1007/bf00740464>.
17. Abbud-Madrid A, Modak A, Branch M C, et al. Combustion of Magnesium with Carbon Dioxide and Carbon Monoxide at Low Gravity. *Journal of Propulsion and Power*, 2001, 17 (4): 852-859. <https://doi.org/10.2514/2.5816>.
18. M.M.Elkothb, N.Salama, I.Nassef. Modeling of Solid Particle Interaction in A High-Velocity, Hot Gas Stream, *Twenty-Sixth Symposium (International) on Combustion/The Combustion Institute*, 1996:1937–1944.
19. Kashireninov O E, Kuznetsov V A , Manelis G B . Kinetics of Alkaline-Earth Atoms Reactions with Molecular Oxygen. *AIAA Journal*, 1971, 15(7):1035-1037. <https://doi.org/10.2514/3.60746>.
20. Wang Song, Combustion of fine magnesium particles, Thesis. 2014.
21. Shoshin Y, Dreizin E. Particle combustion rates in premixed flames of poly disperse metal-air aerosols. *Combustion and Flame*, 2003, 133(3):275-287.
22. H.F. Lehr, Experiments on shock-induced combustion, *Astronaut Acta*, 1972, 17, 589-597.
23. N. Marinov, C.K. Westbrook, W. Pitz, Detailed and global chemical kinetics model for hydrogen, *Proceedings of the Combustion Institute*, 1995, 1.
24. C. Zhuo, F. Feng, X. Wu, Development process of muzzle flows including a gun-launched missile, *Chinese Journal of Aeronautics*. 2015, 28, 385-393. <https://doi.org/10.1016/j.cja.2015.02.001>.
25. M. SOETRISNO, S. IMLAY, Simulation of the flow field of a ram accelerator, *27th Joint Propulsion Conference*, 1991.
26. S. Yungster, S. Eberhardt, A.P. Bruckner, Numerical simulation of hypervelocity projectiles in detonable gases, *AIAA Journal*, 1991, 29, 187-199. <https://doi.org/10.2514/3.10564>.

Disclaimer/Publisher's Note: The statements, opinions and data contained in all publications are solely those of the individual author(s) and contributor(s) and not of MDPI and/or the editor(s). MDPI and/or the editor(s) disclaim responsibility for any injury to people or property resulting from any ideas, methods, instructions or products referred to in the content.